Cement and Concrete Research 41 (2011) 602–608

Contents lists available at ScienceDirect

Cement and Concrete Research

journal homepage: http://ees.elsevier.com/CEMCON/default.asp

A remastered external standard method applied to the quantification of early OPC hydration

Daniel Jansen, Friedlinde Goetz-Neunhoeffer *, Christopher Stabler, Jürgen Neubauer

Mineralogy, GeoZentrum Nordbayern, University of Erlangen-Nuremberg, D-91054 Erlangen, Germany

ARTICLE INFO

Article history:
Received 7 December 2010
Accepted 4 March 2011

Keywords:
Hydration (A)
Kinetics (A)
Amorphous material (B)
X-ray diffraction (B)
Cement paste (C)

ABSTRACT

A promising external standard method, first described by O'Connor [15], was used to determine the quantitative phase composition of a hydrating cement paste. On the basis of the data produced we can conclude that the method used is absolutely to be recommended for the examination of OPC pastes, since it displays many advantages in comparison to internal standard methods and other methods. No reaction of the phase alite could be detected during the initial and the induction periods of the cement hydration. Additionally it was found that the cement phases involved in the aluminate reaction (bassanite, gypsum, anhydrite and C_3A) react successively. The changes detected in the phase composition of the OPC paste could be assigned to the different periods of OPC hydration.

1. Introduction

The hydration of Ordinary Portland Cements (OPCs) is a complex scientific issue. The kinetics behind the hydration process is still a subject of scientific debate. X-ray diffraction (XRD) analysis is a suitable method for examining the hydration process.

Hence, several scientists have published articles in which the quantities of the crystalline phases of cement pastes were measured during the process of hydration. During the early stages of the hydration process, OPCs form portlandite and a C-S-H phase of varying composition [1,2] which is hard to detect by X-ray diffraction because of its low degree of crystallinity. In addition to this, the water added to the cement cannot be quantified directly by means of X-rays and if AFm phase is present it may also have a low degree of crystallinity. During the aluminate reaction, ettringite is formed from calcium sulfate and tricalcium aluminate (C_3A) [3].

Rietveld analysis always gives the total of the crystalline phases as determined, normalized to 100 wt.% (Eq. (1)). If amorphous phases are present (in the case of OPC's at least C-S-H phase and water), then the amounts of crystalline phases calculated by the analysis will differ from the actual amounts present. In addition, any error made in computing any phase (e.g. wrong use of preferred orientation and wrong use of the micro strain) of the mixture will have an impact on the calculated amount of all phases in the mixture. Besides, every unidentified phase will lead to a falsification of the results when using a normalization to 100 wt.%.

$$c_j = \frac{S_j(ZMV)_j}{\sum_{i=1}^{n} S_i(ZMV)_i} \quad (1)$$

where

c_j	Weight fraction of phase j
S_j	Rietveld scale factor of phase j
Z	Number of formula units per unit cell
M	Mass of the formula unit
V	Unit-cell volume.

Several articles have been published describing methods which might possibly be used to avoid the problem of false quantitative results for the crystalline phases in the cement paste.

The problem of false Rietveld results can be overcome by plotting e.g. peak areas [4], normalized peak areas [5] or relative peak intensities [6]. This approach does indeed have certain advantages. The peak areas as well as the peak intensities can show any decrease or increase of phase contents in a cement paste. Since there is here no normalization to 100 wt.%, it can be ensured that there is no falsification of the data caused by the normalization process. No error committed while determining the peak areas or the peak intensities of one phase will necessarily have any impact on the calculated peak areas or peak intensities of the other phases present in the cement paste. Unfortunately, it is not possible to calculate by this method actual quantities given in wt.% of the cement paste.

* Corresponding author. Tel.: +49 9131 85 25780; fax: +49 9131 85 23734.
E-mail addresses: DanHerJansen@googlemail.com (D. Jansen), goetz.gzn@me.com (F. Goetz-Neunhoeffer).

0008-8846/$ – see front matter © 2011 Elsevier Ltd. All rights reserved.
doi:10.1016/j.cemconres.2011.03.004

In order to arrive at the actual phase content of each phase in the cement paste in wt.%, the results obtained via Rietveld analysis can be converted, taking into account the C-S-H phase, free water and bound water [7,8]. Therefore, a fixed chemical composition of the C-S-H phase has to be assumed based on a thinkable reaction of alite with water to portlandite and C-S-H (e.g. Eq. (4), $C_{1.7}SH_{2.6}$) and the amount of C-S-H phase has to be calculated from the amount of portlandite detected. If the assumed chemical composition differs strongly from the actual composition, a systematic error in the phase composition of the cement paste may occur. Any error in the determination of the amount of portlandite will falsify the amount of the C-S-H phase as well.

Other possibilities are standard methods. An internal standard material can be added, in order to arrive at the phase composition of the crystalline phases as well as the amount of the amorphous content of the cement paste (C-S-H phase and water) [9,10]. If an internal standard is added to the cement, it is possible that this standard material will have an impact on the hydration of the cement. Westphal et al. [11] recommend an amount of 40 wt.% of internal standard for a system with approximately 35 wt.% of amorphous content (depends on amount of C-S-H phase and water in a cement paste) in order to minimize the uncertainty of the results for the amorphous content of the sample. The uncertainty is in this case a function of the amount of internal standard added to the sample and is based on mathematical consequences of the internal standard method. An amount of 40 wt.% of internal standard would have an impact on the hydration behavior because of the dilution of the cement phases in the sample. Proper mixing of the standard with the cement has also to be ensured, and issues such as micro-absorption have to be taken into account, especially if the mass attenuation coefficients of sample and standard differ significantly from one another [12].

Recently, it has been shown that the scale factor calculated during Rietveld refinement is also suitable for calculating quantities in the cement paste [13,14].

To avoid complications that might be caused by mixing an internal standard with the OPC used, we decided to make use of an external standard method which was first described by O'Connor [15] but which has not since been used again for the quantification of cement pastes. The method has already been used successfully for the quantification of cements, cement/fly ash-mixtures [17,21] and also organic mixtures [51].

2. Materials and methods

In our experiments we made use of an Ordinary Portland Cement (CEMI 52.5R). To ensure a proper detection of all phases in the OPC used, minor phase enrichment experiments were performed. The dissolution of the interstitial phases by application of KOH solution allows an accurate analysis of the silicate phases, such as alite, belite, and α'-C_2S [18] (Gutteridge, 1979). Conversely, the dissolution of the silicate phases using a salicylic acid–methanol solution allows an accurate analysis of the interstitial phases [19].

As only small amounts of sample are necessary for the XRD experiments performed, representative components for analysis were obtained by using the "cone and quarter" method. In order to acquire the best crystalline material available, we made use of a single silicon crystal produced for wafer production. We carefully ground a piece of said single silicon crystal so as to produce a powder of suitable grain size for the X-ray experiments. These single crystals are known to have a high chemical purity (99.999%), which in turn is important when assuming the right mass attenuation coefficient of the standard. Silicon is a highly symmetric material (cubic; Fd-3mS) which is very well known for its use as a peak position standard material. Because of its brittleness, grinding it for just one minute in a micronizing mill was sufficient to achieve our purposes. We therefore assume that no significant amorphous content was produced during the grinding procedure.

The well known silicon standard used in the study was employed for derivation of factor G using Eq. (2) [15]. Scale factors were obtained from Rietveld refinement [16] using the fundamental parameters approach and the Rietveld-software Topas V4.2. All structures used for the refinement are shown in Table 1.

$$G = s_{Si}\frac{\rho_{Si}V_{Si}^2\mu_{Si}^*}{c_{Si}} \tag{2}$$

where

S_{Si}	Rietveld scale factor of silicon from Rietveld analysis
ρ_{Si}	Density of silicon
V_{Si}	Unit-cell volume of silicon
C_{Si}	Weight fraction of silicon (100 wt.%)
μ^*	Mass attenuation coefficient of silicon.

Since silicon is difficult to handle and to prepare, we made use of the factor G derived from the crystalline silicon in order to calibrate a secondary quartz standard of not exactly known chemical composition (and therefore unknown mass attenuation coefficient) cut from quartzite-rock, which was delivered from Bruker AXS along with the diffractometer which we also used. We made use of the secondary standard quartzite because it does not have to be prepared for every measurement. The calibration of the quartzite was performed with 8 measurements for the silicon and the quartzite respectively. The mean values for the scale factors were used. The standard deviation for the scale factors was 0.8% of the mean values for the scale factors.

The factor G is, among others, a function of the Rietveld scale factor. The scale factor depends also on the performance of the X-ray tube, which tends to suffer a degree of performance loss over time. Fig. 1 shows the development of the scale factor for the standard quartzite material, as delivered from Bruker AXS. It can be seen that the factor G has to be calculated separately for each measurement. If the factor G is calculated at a point in time lying long before the actual measurement of the sample, this will result in an underestimation of the crystalline material and an overestimation of the amorphous content of the sample. For this reason, the period of time allowed to elapse between the time of the measurement of the standard material and that of the measurement of the sample should not amount to more than 7 days.

The factor G as calculated is a calibration constant for the whole experimental set-up and includes the diffractometer set-up used, as well as radiation and all data-acquisition conditions such as temperature (dislocation parameters of the atoms in the structures [21]) and counting time. The factor G arrived at was then used to determine the mass concentration of each phase j in the hydrating

Table 1
Structures used for the Rietveld refinements performed.

Phase	ICSD Code	Reference
Alite (C_3S)	94742	De La Torre et al. [37]
Belite (C_2S)	963	Jost et al. [38]
α'-C_2S	–	Mueller [39]
C_3A_{cubic}	1841	Mondal and Jeffery [40]
$C_3A_{\text{orthorombic}}$	100220	Takéuchi and Nishi [41]
C_4AF	51265	Jupe et al. [42]
Gypsum	27221	Pedersen et al. [43]
Bassanite	380286	Weiss and Bräu [44]
Anhydrite	16382	Kirfel and Will [45]
Calcite	80869	Maslen [46]
Quartz	174	Le Page and Donnay [47]
Arcanite	79777	Ojima et al. [48]
Ettringite	155395	Goetz-Neunhoeffer and Neubauer [49]
Portlandite	34241	Busing and Levy [50]

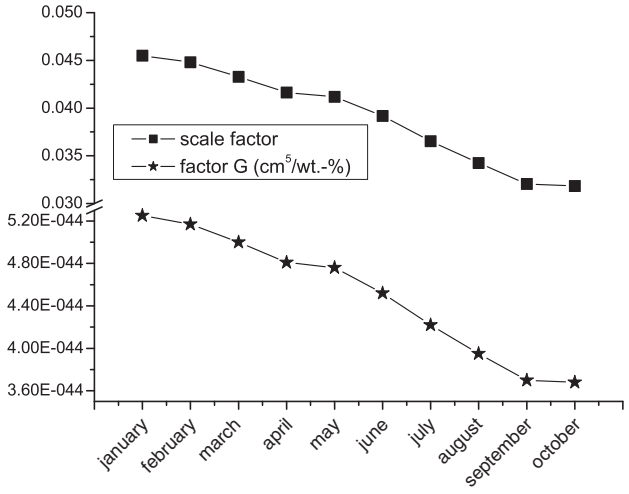

Fig. 1. Change in the scale factor and factor G over time (10 month).

cement paste (Eq. (3)). This made it imperative that the sample be measured under the same conditions as the standard. Since the cement paste was covered, when being measured, with a Kapton film which can cause absorption of X-rays and thereby intensity loss, it was necessary that the standard material be measured and covered with the Kapton film as well. Otherwise the intensities of the standard material might have been misinterpreted, with compensation in the scale factor, thus giving rise to an inaccurate factor G.

$$c_j = s_j \frac{\rho_j V_j^2 \mu^*_{SAMPLE}}{G} \tag{3}$$

The values ρ and V for each phase were computed within the refinement, being checked against data from the literature (data sets from ICSD). Scale factors for the phases detected in the OPC were taken from Rietveld refinement. The mass attenuation coefficient of the OPC μ^*_{OPC} was calculated from elemental analysis measured by X-ray fluorescence spectrometry. The said mass attenuation coefficient of the OPC used was found to be 97.95 cm^2/g, using data for mass attenuation coefficients from the International Tables for Crystallography [20]. Since we made use of a w/c ratio of 0.5, the mass attenuation of the sample μ^*_{SAMPLE} (cement paste) turned out finally to be 68.7 cm^2/g. The chemical composition and the phase composition of the OPC used are given in Table 2. A detailed discussion concerning the amorphous content of Portland cements is given elsewhere [21].

Table 2
Phase composition and chemical composition of the OPC (CEMI 52.5R) used.

Phase	wt.%	Oxide	wt.%
Alite (C_3S)	57.7 +/− 1.2	CaO	66.2
Belite (C_2S)	11.7 +/− 0.6	SiO_2	22.6
α′-C_2S	8 +/− 0.5	Al_2O_3	4.1
C_3A_{cubic}	5.6 +/− 0.3	Fe_2O_3	1.3
$C_3A_{orthorombic}$	4.8 +/− 0.3	MgO	0.8
C_4AF	1.9 +/− 0.2	K_2O	0.7
Gypsum	0.8 +/− 0.1	Na_2O	0.1
Bassanite	1.5 +/− 0.1	SO_3	3.4
Anhydrite	3 +/− 0.2		
Calcite	2.2 +/− 0.2		
Quartz	0.9 +/− 0.1		
Arcanite	0.9 +/− 0.1		
Amorphous/misfitted	1		

For the in-situ XRD analysis a custom-made sample holder was used [22]. Cement and water were mixed by external stirring for one minute, using an electric stirrer which allows a reproducible stirring. The paste was then prepared into the sample holder and covered by a 7.5 μm thick Kapton polyimide film. The diffraction patterns were recorded using a D8 diffractometer (Bruker) equipped with a LynxEye PS-Detector. We made use of CuKα radiation at 40 kV and 40 mA and recorded from 7° 2θ to 40° 2θ with a step width of 0.0236 and 0.58 s, counting time per step. Under these data acquisition conditions, it is possible to record 88 ranges within the first 22 h of hydration. The Rietveld program used was Topas 4.2 from Bruker AXS. The background caused by the Kapton polyimide film was fitted with a specific background model. To this end the Kapton foil was stretched over a single crystal sample holder and the pattern of the Kapton foil was fitted with a peak phase which was later used for the refinement of the cement paste [7].

3. Results

Fig. 2 shows the refined XRD pattern of the cement paste after 22 h of hydration. There is a close agreement between the observed data and the calculated data. At this point in time after the start of hydration there was no sign for AFm phase and the peak of the C-S-H phase was not very distinct.

Fig. 3 shows the alite content over time, within the first 22 h of hydration, from 4 measurements with individual preparation. It can be clearly seen that the results for the phase alite during hydration are reproducible. The results of all other phases were as good as that of the alite in terms of reproducibility. The biggest error occurred regarding the total amount detected. Since we can detect 57.7 wt.% of alite in the dry cement, we can assume about 38 wt.% in the cement paste (w/c = 0.5), if no alite reacts immediately after mixing the cement with water. Fig. 3 shows that we can indeed find that amount in the first XRD pattern of the hydrating cement paste, considering the single standard deviation from 1 wt.% of our experiments. Therefore, we cannot prove that alite dissolves immediately with water, forming C-S-H and portlandite. In addition, we cannot detect portlandite in the first XRD patterns.

Fig. 4 shows the heat flow, as measured, of the OPC used, as well as the phase development of the phases alite and portlandite. It can be clearly seen that the alite dissolution, as well as the portlandite precipitation, begins at the end of the induction period (beginning of the acceleration period), this being, in our case, 2.5 h after the beginning of hydration. At the beginning of the acceleration period, we can detect the beginning of the dissolution of alite, as well as the precipitation of portlandite, both taking place synchronously.

It can be shown that the reaction assumed for the silicate reaction (Eq. (4)) runs synchronously, which means that the dissolution of the phase alite occurs at the same time as the precipitation of the phase portlandite. Since the C-S-H phase cannot be detected by XRD-methods, it has to be assumed that the precipitation of the C-S-H phase occurs at the same time as the precipitation of the phase portlandite.

$$C_3S + 3.9H_20 \rightarrow C_{1.7}SH_{2.6} + 1.3Ca(OH)_2 \tag{4}$$

In the experiments performed there was no sign for the reaction of the phase belite. These findings correspond to findings from the literature [52].

According to Eq. (4), the consumption of 1 mol of C_3S can result in the precipitation of 1.3 mol of portlandite. If we take the molar masses into account, this means that we need 237.1 g of C_3S to precipitate 100 g of portlandite (ignoring the possibility of incorporation of other ions). The ratio between C_3S consumed and portlandite precipitated should, ideally, be 2.37. Our calculated ratio of around 2.53 (Eq. (5)) after 22 h hydration agrees almost exactly with the theoretical value.

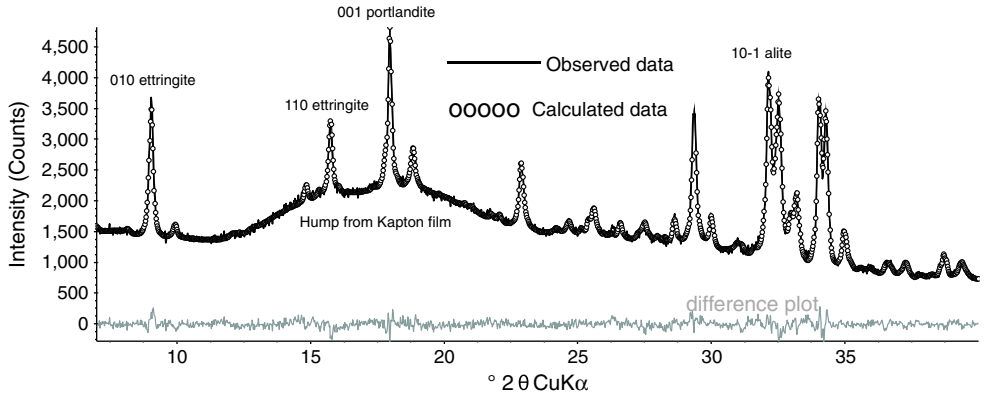

Fig. 2. Refined pattern of the cement paste at 23 °C and w/c = 0.5 after 22 h hydration.

Where we take into account the single standard deviation of 1 wt.% from Rietveld analysis, we arrive at an absolutely exact agreement with the theoretical value of 2.37.

$$\frac{\Delta\, alite_{22h}}{\Delta\, portlandite_{22h}} = \frac{20\, wt.\%}{7.9\, wt.\%} = 2.53 \tag{5}$$

where

$\Delta alite_{22h}$ dissolved amount of alite after 22 h hydration [wt.%]
$\Delta portlandite_{22h}$ precipitated amount of portlandite after 22 h hydration [wt.%].

Fig. 5 shows the heat flow curve of the cement examined and the cement phases involved in the aluminate reaction, which react to the hydrate phase ettringite during hydration. Since we find 3 wt.% of anhydrite in the dry cement, we can assume the presence of 2 wt.% of anhydrite in the cement paste (w/c = 0.5) if no anhydrite reacts within the first minutes of hydration. We find almost 2 wt.% of anhydrite in the first measurement of the cement paste. Additionally we observe a reaction of the phase anhydrite within the first 2.5 h of hydration. At point 1, the first dissolution of anhydrite is completed and we can detect the dissolution of the phase gypsum. We cannot prove a dissolution of gypsum immediately after mixing the cement with water. Since 0.8 wt.% of gypsum is detected in the dry cement, 0.5 wt.% of gypsum can be assumed to be present in the cement paste, supposing a w/c ratio of 0.5, if no gypsum reacts within the first minutes. Since we find about 0.5 wt.% in the cement paste over the first 4 h, we can assume that gypsum does not react at any rapid rate in the cement system examined.

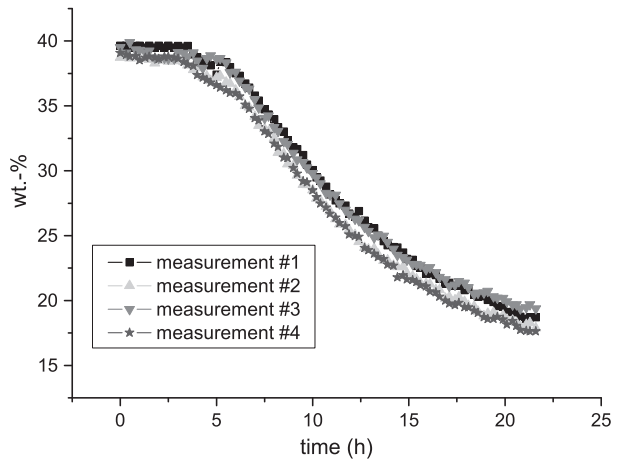

Fig. 3. Alite content during hydration of the OPC used at 23 °C, using a w/c ratio of 0.5.

There are two other sulfate containing phases in the dry cement, namely bassanite and arcanite. Neither phase could be detected in the first XRD patterns of the cement paste. Therefore, we can assume that both phases react immediately with the mixing water and provide a high sulfate concentration in the pore solution for the first ettringite precipitation.

At point 2, the dissolution of the phase gypsum is completed and a second dissolution of the phase anhydrite can be detected. At point 3 the dissolution of the phase anhydrite is retarded and a further reaction of the C_3A can be detected.

Furthermore, we can detect a disparity between the amount of C_3A expected from the analysis of the dry cement and the amount of C_3A actually detected in the first recorded pattern of the cement paste, namely, about 2 wt.% +/−0.5 wt.% (Fig. 5). Due to the molar masses of C_3A and ettringite we can assume that 2 wt.% of C_3A can lead to the formation of about 9 wt.% of ettringite, when we take into account the following reaction for the precipitation of ettringite.

$$C_3A + 3CaSO_4 + 32H_2O \rightarrow C_3A * 3CaSO_4 * 32H_2O\ (\text{Ettringite}). \tag{6}$$

The said 9 wt.% +/−0.5 wt.% is approximately equal to the amount of ettringite we can detect at 12.5 h after the beginning of hydration, which is also the point within the hydration process at which the further dissolution of C_3A begins to occur, synchronously with an accelerated precipitation of ettringite (Fig. 6). There was no sign for the reaction of the C_4AF in the first 22 h of hydration. We assume that the alumina of the dissolved alite is incorporated in the C-S-H phase [53].

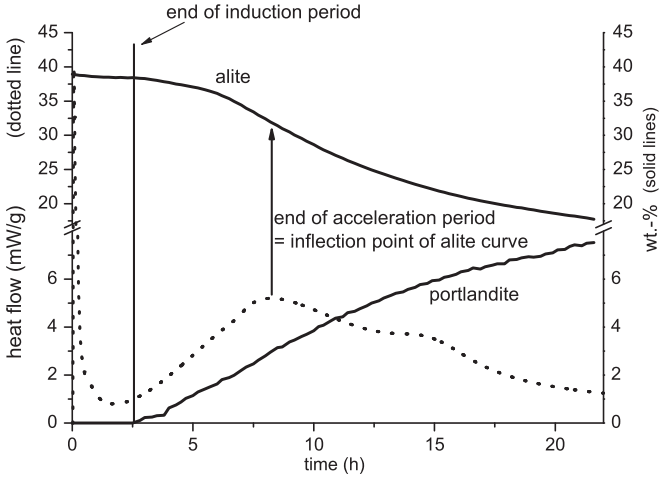

Fig. 4. Alite content, portlandite content and measured heat flow during the hydration of the OPC used at 23 °C, using a w/c ratio of 0.5.

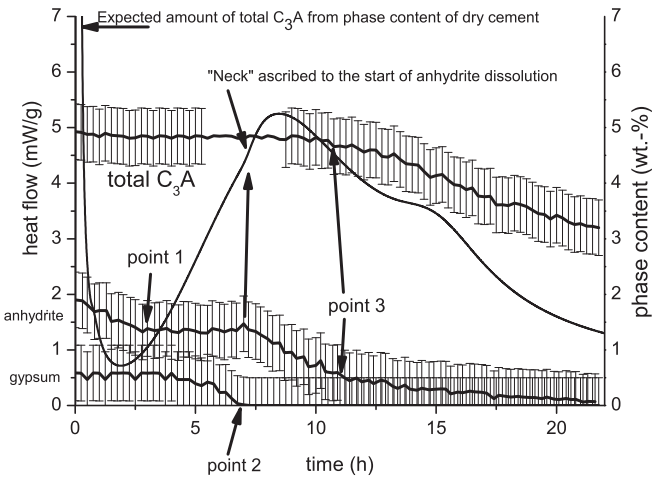

Fig. 5. C_3A content, anhydrite content, gypsum content and measured heat flow during the hydration of the OPC used at 23 °C, using a w/c ratio of 0.5.

We can confirm the assumption of Hesse et al. [13] that there may exist an amorphous aluminate phase which can serve as a reservoir for further ettringite formation. Indeed, 27 Al NMR experiments might be interesting to perform in order to describe the assumed Al-reservoir.

We also detect that the cement phases involved in the aluminate reaction react successively (Fig. 5). Firstly, the phases arcanite and bassanite are not detectable in the first scan of the paste. The lack of the phases reflects the fast dissolution of both phases. Additionally, we detect an initial dissolution of the phase anhydrite immediately after mixing the cement with water. Up until a point in time of 2.5 h after the beginning of hydration an ongoing dissolution of the phase anhydrite is detected. The dissolution of the anhydrite is interrupted during the dissolution of the phase gypsum. Dissolution of the phase anhydrite only begins once again when the dissolution of the phase gypsum has been completed. At about 12 h after the beginning of the hydration process we observe a retarded dissolution of the phase anhydrite, the last available sulfate carrier, and consequently the further reaction of C_3A. No synchronous dissolution of two phases like anhydrite and gypsum, or of any sulfate carrier and C_3A, can be detected within the first 22 h of hydration. Bassanite is the most soluble sulfate carrier with a solubility of about 8 g/L at ambient conditions whereby the solubilities of gypsum and anhydrite are more similar to one another (between 2.3 g/L and 2.8 g/L). We assume that the cement used contains anhydrite of different solubilities dependent on grain size,

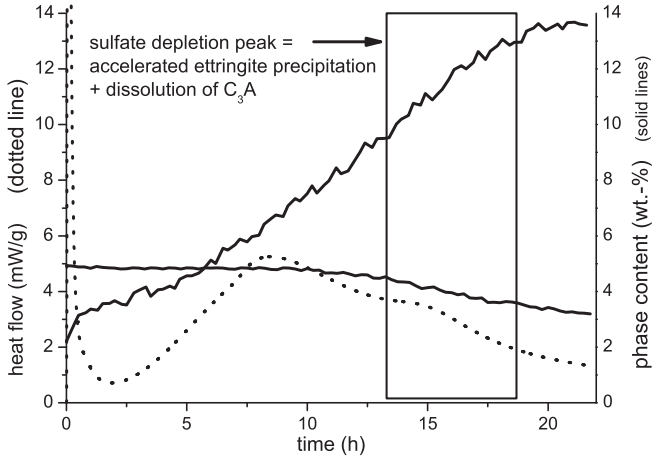

Fig. 6. Ettringite content, C_3A content and measured heat flow during the hydration of the OPC used at 23 °C, using a w/c ratio of 0.5.

degree of crystallinity and surface defects. The most soluble anhydrite reacts before the gypsum up until point 1, a less soluble anhydrite reacts after the complete dissolution of the phase gypsum after point 2, and the least soluble anhydrite reacts after point 3.

Both the reaction of the aluminate and the accelerated precipitation of ettringite cause the significant 2nd local heat flow maximum at about 15 h after the start of hydration – a phenomenon which had also been ascribed to the aluminate reaction by Hesse et al. [13] – thereby confirming the findings of Lerch [23] which described this maximum as a function of sulfate depletion. At the end of our examinations at 22 h after the beginning of hydration an amount of ettringite of about 13.5 wt.% had been formed in the cement paste. The sulfate content of our cement is 3.4 wt.% which corresponds to 2.3 wt.% in the cement paste. Since some 0.5 wt.% of anhydrite failed to react during the first 22 h, around 0.2 wt.% of the SO_3-content of the cement were not available for the ettringite precipitation. According to Eq. (6), around 11 wt.% of pure sulfate ettringite can be formed with the said amount of sulfate. A disparity between the amount of ettringite calculated from the sulfate content of the cement (11 wt.%) and the amount detected (13.5 wt.%) can be observed. The phenomenon of formation of solid solutions during the hydration of ettringite has been described by several authors [24–26]. But considering the findings of Renaudin et al. [27], which showed that there is a significant variation in the lattice parameters of pure sulfate-ettringite depending on humidity, it is not possible to make statements concerning the chemical composition of the ettringite based on the refinement of the lattice parameters in wet cement pastes. Therefore, a slight enrichment of ettringite at the contact point of the cement paste and Kapton foil in addition to the uncertainties of the measurements are the most obvious explanation for the slight overestimation of the phase ettringite.

4. Discussion

Different hypotheses exist concerning the hydration kinetics of Portland cements and the phases present in OPCs. These were reviewed by Bullard et al. [28] and also by Juilland et al. [29], who worked out that the dissolution theory can explain the early hydration behavior of alite without having to invoke the formation of a metastable barrier. It has recently been described, however, how the formation of shells around cement grains tends to limit reaction behavior [30]. It was shown by Gallucci et al. that there is no sign of a reaction of the phase alite during cement hydration over the first hours of cement hydration. The formation of shells around the grains occurs during and at the end of the induction period. In accordance with these findings, we must conclude that we cannot prove any reaction of alite during the initial reaction and the induction period. It had been shown by Juilland et al. [29] that there is no sign of a reaction of the phase alite in saturated lime solutions. It is conceivable that the rapid reaction of the C_3A, as well as the reaction of the sulfate carriers arcanite and bassanite, cause a pore solution composition which prevents the initial dissolution of the phase alite.

Studies have shown that the C-S-H nucleation and growth restrict the early age hydration during the acceleration period. According to Bullard et al. [31] the growth of the C-S-H phase, respectively the nucleation and the number of active growth sites, is rate controlling. Thomas et al. [32] have shown that the seeding of cement pastes with reactive C-S-H phases at the time of mixing causes an acceleration of the hydration and results in the induction period's being almost entirely eliminated. These findings agree with our findings in the acceleration period. During the acceleration period we detected an increasing reaction rate of alite over time. If we assume that we have increasing numbers of active growth sites during the acceleration period, we can explain a more rapid precipitation of the hydrates and, consequently, a more rapid reaction of alite over time.

The point of inflection in the dissolution curve of alite corresponds to the heat flow maximum, occurring at about 9 h, in the heat flow

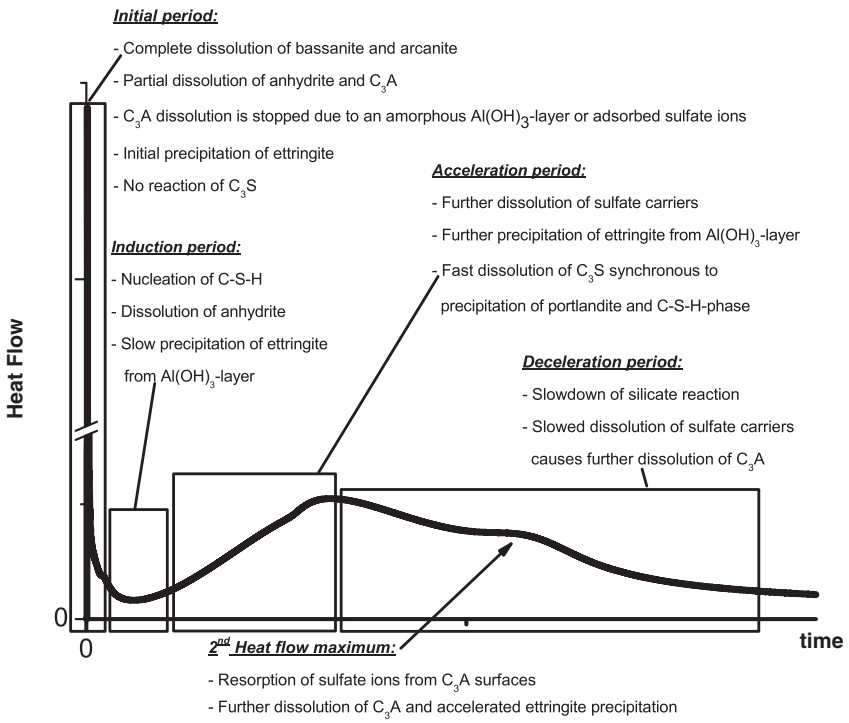

Fig. 7. Changes detected in the phase composition of the OPC paste, assigned to the different periods of OPC hydration.

curve of the cement used (Fig. 4). It can be assumed that after 9 h the rate controlling mechanism changes and the deceleration period is reached. During that period we observe a decreasing reaction rate of alite dissolution. This might be caused by either lack of space or lack of water. Furthermore, it has been debated whether the controlling factor during the cement hydration may be the diffusion of the ions through the pore solution. Another interesting hypothesis to explain the decreasing reaction rate during the deceleration period has been suggested by Thomas et al. [33] who worked out that the intergrowth of the hydration products leads to a decreasing number of active growth sites, which in turn leads to that decreasing reaction rate of the phases in the cement paste which we detected with our XRD in-situ experiments.

Synchronous to the silicate reaction there also occurs the aluminate reaction, with the formation of ettringite. On the basis of the data produced, we can confirm that there is a very rapid reaction of the C_3A at the beginning of the hydration process. In addition, a rapid dissolution of the sulfate-containing phases bassanite, arcanite and anhydrite is detected, with bassanite and arcanite reacting faster than anhydrite. The retardation of any further reaction of C_3A seems to be caused by the presence of the sulfate carriers. As long as sulfate carriers are present we cannot prove a further dissolution of C_3A. Scrivener and Pratt [34] have pointed out that the morphology of ettringite as hexagonal rods is unlikely to provide any barrier to the C_3A capable of inhibiting ion transport. Therefore, it seems unlikely that the hydration product of C_3A, ettringite, forms a barrier on the surfaces of the C_3A.

The C_3A surfaces have a positive charge in solution [35]. The adsorption of ions from solution on surfaces is a function of charge density. The sulfate ions are comparatively small, with two charges. Therefore, an adsorption of the sulfate ions on the surfaces of the C_3A is conceivable. This possibility has in fact also been discussed, namely by Minard et al. [36]. It is not clear whether the adsorption of the sulfate ions on the surfaces of the C_3A causes the cessation of the C_3A dissolution or whether it is rather the composition of the pore solution (high concentration of sulfate ions) which inhibits the further reaction of the C_3A. Moreover, it is also possible that the assumed amorphous layer, which can be seen as an Al-reservoir for ettringite precipitation, might inhibit further dissolution of C_3A.

Synchronous to the local heat flow maximum, at about 15 h into the hydration process of the OPC which we used, there is a detected rapid precipitation of ettringite as well as further hydration of C_3A. The aluminate hydration product is still ettringite, not calcium monosulfoaluminate. Previous to this, there is an observed less rapid dissolution of the phase anhydrite, which is the last sulfate carrier present. We ascribe the less rapid reaction of the anhydrite to the less reactive nature of the anhydrite grains, which might either be bigger than the more reactive ones or might have a higher degree of crystallinity. The beginning of the anhydrite dissolution can be tracked in the heat flow diagrams during the acceleration period. At about 7.5 h after the start of hydration process, a distinct “neck” in the heat flow curve of the cement can be observed. This can be ascribed to the onset of the anhydrite dissolution (Fig. 5). After about 12 h, the slower reaction of the anhydrite causes a slump of the sulfate ions in the pore solution. A desorption of the sulfate ions from the surfaces of the C_3A into the pore solution results in a more rapid availability of sulfate, as well as a further reaction of the C_3A. Both reactions, which occur synchronously, permit a faster precipitation of ettringite than before. As soon as the available sulfate has been consumed for ettringite precipitation the final precipitation of the ettringite is concluded.

5. Conclusion

The implementation of the method using a factor G presented in this paper offers a lot of advantages. Firstly, the concentration of each phase can be detected directly from the scale factor. Secondly, any errors made in Rietveld quantification will not, where this method is used, necessarily have an impact on the other phases present in the OPC paste. Lastly, the difference between the total of crystalline phases and 100 wt.% can be attributed directly to the amorphous components in the OPC paste, i.e. not to crystalline bounded water and C-S-H phase. This means that the amorphous content of the cement paste during hydration can be measured indirectly. On the

basis of the data produced, a hydration model for the early hydration of OPC can be assumed (Fig. 7).

6. Future perspectives

The method presented is very promising for the quantitative study of cement hydration. There are many other fields within construction chemistry in which the method presented here looks likely to prove very useful. In ternary systems containing Portland cements and calcium aluminate cements (CAC), more than one amorphous phase is formed in addition to the added water. In this case, an external standard method is the most promising method available. The very rapid reaction of crystalline phases immediately after the mixing of the binder with the water can be examined by comparing the quantification of the dry binder with the first XRD patterns of the hydrating pastes.

References

[1] J.I. Escalante-Garcia, J.H. Sharp, Variation in the composition of C-S-H gel in Portland cement pastes cured at various temperatures, J. Am. Ceram. Soc. 82 (1999) 1131–1147.
[2] I.G. Richardson, The calcium silicate hydrates, Cement Concr. Research 38 (2008) 137–158.
[3] H.F.W. Taylor, Cement Chemistry, 2nd ed, Thomas Telford Publishing, 1997.
[4] H. Pöllmann, M. Fylak, R. Wenda, Investigations on hydration reactions and hydration behavior of cements and cement phases, Tagungsbericht 17, Int. Baustofftagung Weimar Band 1 (2009) 1–0161-1-0176.
[5] A. Quennoz, E. Gallucci, C.F. Dunant, K.L. Scrivener, Influence of the gypsum amount on the hydration of tricalcium aluminate in C_3A-gypsum and alite-C_3A-gypsum systems, Tagungsbericht 17, Int. Baustofftagung Weimar Band 1 (2009) 1–0207-1-0212.
[6] L. Pelletier, F. Winnefeld, B. Lothenbach, Hydration mechanism of the ternary system Portland cement – calcium sulphoaluminate – anhydrite, Tagungsbericht 17, Int. Baustofftagung Weimar Band 1 (2009) 1–0277-1-0282.
[7] C. Hesse, F. Goetz-Neunhoeffer, J. Neubauer, M. Braeu, P. Gaeberlein, Quantitative in situ X-ray diffraction analysis of early hydration of Portland cement at defined temperatures, Powder Diffr. 24 (2009) 112–115.
[8] D. Jansen, F. Goetz-Neunhoeffer, J. Neubauer, W.-D. Hergeth, R. Haerzschel, Influence of polyvinyl alcohol on phase development during the hydration of Portland cement, ZKG Int. 7 (2010) 100–107.
[9] K.L. Scrivener, T. Füllmann, E. Gallucci, G. Walenta, E. Bermejo, Quantitative study of Portland cement hydration by X-ray diffraction/Rietveld analysis and independent methods, Cem. Concr. Res. 34 (2004) 1541–1547.
[10] L.D. Mitchell, J.C. Margeson, P.S. Whitfield, Quantitative Rietveld analysis of hydrated cementitious systems, Powder Diffr. 21 (2006) 111–113.
[11] T. Westphal, T. Füllmann, H. Pöllmann, Rietveld quantification of amorphous portions with an internal standard — mathematical consequences of the experimental approach, Powder Diffr. 24 (2009) 239–243.
[12] H. Hermann, M. Ermrich, Microabsorption correction of X-ray intensities diffracted by multiphase powder specimens, Powder Diffr. 4 (1989) 189–195.
[13] C. Hesse, F. Goetz-Neunhoeffer, J. Neubauer, A new approach in quantitative in-situ XRD of cement pastes: correlation of heat flow curves with early hydration reactions, Cem. Concr. Res. 41 (2010) 123–128.
[14] M. Merlini, G. Artioli, T. Cerulli, A. Bravo, F. Cella, Tricalcium aluminate hydration in additivated systems, crystallographic study by SR XRPD Cement Concr. Res. 38 (2008) 477–486.
[15] B.H. O'Connor, M.D. Raven, Application of the Rietveld refinement procedure in assaying powdered mixtures, Powder Diffr. 3 (1988) 2–6.
[16] H.M. Rietveld, A profile refinement method for nuclear and magnetic structures, J. Appl. Crystallogr. 2 (1969) 65–71.
[17] J. Neubauer, S. Dittrich, F. Goetz-Neunhoeffer, D. Jansen, Quantitative analysis of OPC, fly ash and mixtures, monograph of the congress on building chemistry, Dortmund (2010) 85–92.
[18] W.A. Gutteridge, On the dissolution of the interstitial phases in Portland cement, Cem. Concr. Res. 9 (1979) 319–324.
[19] L.J. Struble, The effect of water on maleic acid and salicylic acid extractions, Cem. Concr. Res. 15 (1985) 631–636.
[20] International Union for Crystallography, Prince, E., International Tables for Crystallography, Volume C: Mathematical Physical and Chemical Tables, third edition, Wiley, 2004.
[21] D. Jansen, C.h. Stabler, F. Goetz-Neunhoeffer, S. Dittrich, J. Neubauer, Does Ordinary Portland Cement contain amorphous phase? A quantitative study using an external standard method, Powder Diffr. 26 (2011) 31–38.
[22] C. Hesse, M. Degenkolb, P. Gäberlein, F. Goetz-Neunhoeffer, J. Neubauer, V. Schwarz, Investigation into the influence of temperature and w/c-ratio on the early hydration of white cement, Cement Int. 6 (2008) 68–78.
[23] W. Lerch, The influence of gypsum on the hydration and properties of Portland cementpastes, Am. Soc. Test. Mater. 46 (1946) 1252–1297.
[24] H. Poellmann, H.-J. Kuzel, Solid solution of ettringite part I, Cem. Concr. Res. 20 (1990) 941–947.
[25] S.J. Barnett, C.D. Adam, A.R.W. Jackson, An XRPD profile fitting investigation of the solid solution between ettringite $Ca_6Al_2(SO_4)_3(OH)_{12}*26H_2O$ and carbonate ettringite $Ca_6Al_2(CO_3)_3(OH)_{12}*26H_2O$, Cem. Concr. Res. 31 (2001) 13–17.
[26] G. Möschner, B. Lothenbach, F. Winnefeld, A. Ulrich, R. Figi, R. Kretzschmar, Solid solution between Al-ettringite and Fe-ettringite $(Ca_6[Al_{1-x}Fe_x(OH)_6]_2(SO_4)_3*26H_2O)$, Cem. Concr. Res. 39 (2009) 482–489.
[27] G. Renaudin, Y. Filinchuk, J. Neubauer, F. Goetz-Neunhoeffer, A comparative study of wet and dried ettringite, Cem. Concr. Res. 40 (2010) 370–375.
[28] J.W. Bullard, H.M. Jennings, R.A. Livingston, A. Nonat, G.W. Scherer, J.S. Schweitzer, K.L. Scrivener, J.J. Thomas, Mechanisms of cement hydration, Cem. Concr. Res. in press. Corrected Proof, Available online 29 October 2010, ISSN 0008–8846, doi:10.1016/j.cemconres.2010.09.011.
[29] P. Juilland, E. Gallucci, R. Flatt, K. Scivener, Dissolution theory applied to the induction period in alite hydration, Cem. Concr. Res. 40 (2010) 831–844.
[30] E. Gallucci, P. Mathur, K. Scrivener, Microstructural development of early age hydration shells around cement grains, Cem. Concr. Res. 40 (2010) 4–13.
[31] J.W. Bullard, A determination of hydration mechanisms for tricalcium silicate using a kinetic cellular automaton model, J. Am. Ceram. Soc. 91 (2008) 2088–2097.
[32] J.J. Thomas, H.M. Jennings, J.J. Chen, Influence of nucleation seeding on the hydration mechanisms of tricalcium silicate and cement, J. Phys. Chem. C 113 (11) (2009) 4327–4334.
[33] J.J. Thomas, J.J. Biernacki, J.W. Bullard, S. Bishnoi, J.S. Dolado, G.W. Scherer, A. Luttge, Modeling and simulation of cement hydration kinetics and microstructure development, Cem. and Concr. Res. in press. Corrected Proof, Available online 2 February 2011, ISSN 0008–8846, doi:10.1016/j.cemconres.2010.10.004.
[34] K.L. Scrivener, P.L. Pratt, Microstructural studies of the hydration of C_3A and C_4AF independently and in cement paste, in: F.P. Glasser (Ed.), Brit. Ceram. Proc. 35, Stoke-on-Trent, British Ceramic Society, 1984, pp. 207–219.
[35] J. Plank, Ch. Hirsch, Impact of zeta potential of early cement hydration phases on superplasticizer adsorption, Cem. Concr. Res. 37 (2007) 537–542.
[36] H. Minard, S. Garrault, L. Regnaud, A. Nonat, Mechanisms and parameters controlling the tricalcium aluminate reactivity in the presence of gypsum, Cem. Concr. Res. 37 (2007) 1418–1426.
[37] A.G. De La Torre, S. Bruque, J. Campo, M.A.G. Aranda, The superstructure of C_3S from synchrotron and neutron powder diffraction and its role in quantitative phase analysis, Cem. Concr. Res. 32 (2002) 1347–1356.
[38] K.H. Jost, B. Ziemer, R. Seydel, Redetermination of the structure of β-dicalcium silicate, Acta Crystallogr, Sect. B Struct. Crystallogr. Cryst. Chem. 33 (1977) 1696–1700.
[39] R. Mueller, Stabilisierung verschiedener Dicalciumsilikat-Modifikationen durch den Einbau von Phosphat: Synthese, Rietveld-analyse, Kalorimetrie, Diplomthesis (2001) University of Erlangen.
[40] P. Mondal, J. Jeffery, The crystal structure of tricalcium aluminate, $Ca_3Al_2O_6$, Acta Crystallogr, Sect. B Struct. Crystallogr. Cryst. Chem. 31 (1975) 689–697.
[41] Y. Takéuchi, F. Nishi, Crystal-chemical characterization of the Al_2O_3-Na_2O solid-solution series, Z. Kristallogr. 152 (1980) 259–307.
[42] A.C. Jupe, J.K. Cockcroft, P. Barnes, S.L. Colston, G. Sankar, C. Hall, The site occupancy of Mg in the brownmillerite structure and its effect on hydration properties: an X-ray/neutron diffraction and EXAFS study, J. Appl. Crystallogr. 34 (2001) 55–61.
[43] B.F. Pedersen, Neutron diffraction refinement of the structure of gypsum, Acta Crystallogr. Sect. B Struct. Crystallogr. Cryst. Chem. 38 (1982) 1074–1077.
[44] H. Weiss, M.F. Bräu, How much water does calcined gypsum contain? Angew. Chem. Int. Ed. 48 (2009) 3520–3524.
[45] A. Kirfel, G. Will, Charge density in anhydrite $CaSO_4$, from X-ray and neutron diffraction measurements, Acta Crystallogr. Sect. B Struct. Crystallogr. Cryst. Chem. 36 (1980) 288–2890.
[46] E.N. Maslen, V.A. Streltsov, N.R. Streltsova, Electron density and optical anisotropy in rhombohedral carbonates. III. Synchroton X-ray studies of CaCO3, MgCO3 and MnCO3, Acta Crystallogr. Sect. B Struct. Sci. 51 (1995) 929–939.
[47] Y. Le Page, G. Donnay, Refinement of the crystal structure of low-quartz, Acta Crystallogr. Sect. B Struct. Crystallogr. Cryst. Chem. 32 (1976) 2456–2459.
[48] K. Ojima, Y. Hishihata, A. Sawada, Structure of potassium sulfate at temperatures from 296 K down to 15 K, Acta Crystallogr, Sect. B Struct. Sci. 51 (1995) 287–293.
[49] F. Goetz-Neunhoeffer, J. Neubauer, Refined ettringite structure for quantitative X-ray diffraction analysis, Powder Diffr. 21 (2006) 4–11.
[50] W.R. Busing, H.A. Levy, Neutron diffraction study of calcium hydroxide, Acta Crystallogr, Sect. B Struct. Sci. 42 (1986) 51–55.
[51] M. Schreyer, L. Guo, M. Tjahjono, M. Garland, Three approaches to total quantitative phase analysis of organic mixtures using an external standard, J. Appl. Crystallogr. 44 (2011) 17–24.
[52] I. Jelenic, A. Bezjak, M. Bujan, Hydration of B_2O_3-stabilized α′- and β-modifications of dicalcium silicate, Cem. Concr. Res. 8 (1978) 173–180.
[53] I.G. Richardson, G.W. Groves, The incorporation of minor and trace elements into calcium silicate hydrate (C-S-H) gel in hardened cement pastes, Cem. Concr. Res. 23 (1993) 131–138.